Journal of Thermal Analysis and Calorimetry, Vol. 61 (2000) 425–436

REVERSIBLE, THERMALLY INDUCED DOMAIN UNFOLDING IN OLIGOMERIC PROTEINS
Spectral and DSC measurements

A. Ginsburg[*]

Section on Protein Chemistry, Laboratory of Biochemistry, National Heart, Lung and Blood Institute, National Institutes of Health, Bldg 3, Room 208, Bethesda, Maryland 20892-0342, USA

Abstract

Spectral and differential scanning calorimetry (DSC) results for three oligomeric proteins are briefly reviewed. (A) Reversible, thermally-induced partial unfolding reactions in dodecameric glutamine synthetase from *E. coli* involve cooperative, two two-state transitions of subunits and demonstrate communication among subunits. (B) Thermal unfolding of intact *Acanthamoeba* myosin II is more cooperative than that of mammalian skeletal muscle myosin. Nucleotide-induced conformational changes thermally stabilize head domains in both myosins. The long dimeric coiled-coil rod of *Acanthamoeba* myosin II undergoes a reversible, cooperative, single two-state thermal transition with concomitant chain dissociation. (C) The amino terminal domain of enzyme I of the *E. coli* PEP:sugar phosphotransferase system is destabilized by phosphorylation of the active-site His 189.

Keywords: *Acanthamoeba* myosin II rod coiled-coil, amino terminal domain of enzyme I of the phosphoenolpyruvate:sugar phosphotransferase system of *E. coli*, circular dichroism, differential scanning calorimetry, dodecameric glutamine synthetase, oligomeric protein domains, thermal unfolding, UV-spectra

Introduction

Brief reviews of our spectral and DSC results for three protein systems (separately introduced) are presented. These illustrate different aspects of protein–protein interactions as revealed by calorimetric analysis.

A small endothermic enthalpy for reversible, partial unfolding of dodecameric glutamine synthetase from *E. coli* is measurable only because a high degree of cooperativity among subunits exists. In fact, partial unfolding reactions of two subunit domains with different T_m values are linked to those of all twelve identical subunits.

The thermal unfolding of *Acanthamoeba* myosin II occurs over a narrower temperature range than that of mammalian skeletal muscle myosin even though the overall structures of these myosins are similar and nucleotide binding thermally stabilizes

* Fax: (301) 496-0599; E-mail: AOG@cu.nih.gov

1418–2874/2000/ $ 5.00

Akadémiai Kiadó, Budapest
Kluwer Academic Publishers, Dordrecht

globular head domains in both cases. The myosin II rod is an α-helical coiled-coil dimer (~150 000 M_r) and reversibly unfolds in a two-state process with concomitant chain dissociation. The approach to equilibrium for unfolding and folding reactions of the myosin II coiled-coil rod at transition temperatures is slow and requires scan rates of ≤5°C h^{-1} to yield reliable thermodynamic parameters. We have observed also that a local disruption in the helical structure is not necessarily sufficient to establish independent, thermodynamic unfolding domains.

Also described is an unusual situation in which the thermal hydrolysis of the active-site phospho-His 189 in the amino terminal domain of enzyme I of the *E. coli* PEP:sugar phosphotransferase system increases the conformational stability of this domain. Consecutive DSC scans of the reversible unfolding of the enzyme I amino terminal domain first detected this conversion. For intact enzyme I (with C- and N-terminal domains having T_m values of ~41 and 54°C, respectively), an ultra-sensitive DSC is required for scanning at low protein concentrations (~0.15 mg ml^{-1}) to minimize aggregation of unfolded species. Recent spectral and DSC studies indicate that the overall reversibility for thermal unfolding of enzyme I is improved also by adding the reducing agent tris(2-carboxyethyl)phosphine, which protects C-terminal domain thiol groups against oxidation without interference in DSC measurements.

Reversible, partial unfolding of glutamine synthetase from *E. coli*

Glutamine synthetase (GS) is an essential enzyme in the nitrogen metabolism of enteric bacteria, and its activity in synthesizing *L*-glutamine from *L*-glutamate, ATP, and ammonia is strictly regulated both genetically and metabolically [1, 2]. GS from *E. coli* is a large metalloenzyme (622 000 M_r) consisting of twelve identical subunits [3, 4] arranged in two superimposed hexagonal rings [5] with the twelve active sites located at the interface between adjacent subunits within a ring [6, 7]. The larger C-terminal domain of each subunit contains the two active site metal ions, n_1 and n_2 [8, 9] as well as the binding site for *L*-glutamate (*L*-glutamine). ATP spans the adjacent C- and N-terminal domains by binding near Lys-47 [10] and Mn^{2+} at the n_2 site [8, 11]. The N-terminal domain of each subunit is fairly exposed and contains the Trp-57 loop and no tyrosyl residues [7]. The X-ray crystal structural analysis also shows that the stability of contacts between subunits in opposing rings mainly is provided by the carboxyl terminus helical 'thong' which inserts into a hydrophobic pocket formed by two neighbouring subunits on the opposite ring [6, 7]. Intra- and inter-ring hydrogen bonded β-sheet interactions between subunits also stabilize the quaternary structure [7].

Evidence for temperature-induced, reversible transitions of two domains in GS was obtained by monitoring Trp and Tyr exposures spectrally [12]. Thermal transitions were found by Shrake *et al.* [12] to involve the exposures of ~0.7 Trp of the 2 Trp/subunit and ~2 of the 17 Tyr/subunit with each spectral progress curve conforming to a two-state model of partial unfolding (Fig. 1). The exposure of Trp oc-

curred at 2–3°C lower temperatures than that of Tyr. These studies yielded $T_{1/2}$ and ΔH_{vH} values for thermally induced changes in Trp and Tyr exposures, but gave no information on the sizes of the cooperative units undergoing partial unfolding. Subsequent DSC studies indicated that cooperative interactions link partial unfolding reactions of all enzyme subunits [13, 14].

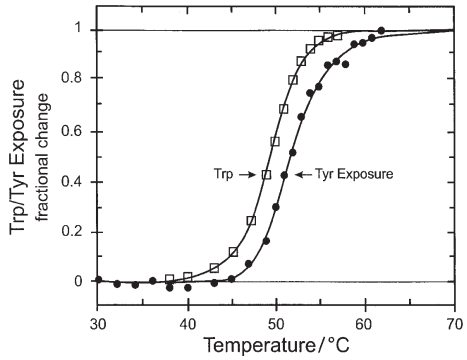

Fig. 1 Normalized progress curves for temperature-induced Trp and Tyr residue exposure during reversible, partial unfolding of dodecameric Mn·glutamine synthetase in 100 mM KCl and 1.0 mM $MnCl_2$ at pH 7.0 (at T_m), using either a random or sequential model for two two-state transitions [12]. For Trp exposure, $T_{1/2}$=50.0°C and for Tyr exposure $T_{1/2}$=51.6°C

A single endotherm for Mn·GS in the presence of 1.0 mM free Mn^{2+} and 100 mM KCl at pH 7.0 was observed by DSC (from 15 to 68°C), with a small positive ΔC_p of 44±4 kJ K^{-1} mol^{-1} [13]. After subtracting the buffer base line, both pre- and post-transitional base lines were linear and these were connected by a progress curve (spanning ΔC_p) which was subtracted from the endothermic peak for data analysis (Fig. 2). Deconvolutions of DSC data were performed [13] using software based on the procedures developed by Freire and Biltonen [15, 16]. The dodecameric structure was retained throughout heating cycles, and thermal transitions were reversible with >93% recovery of activity [13]. A cooperative ratio $\Delta H_{cal}/\Delta H_{vH}$ of 1.6±0.1 and deconvolution analysis showed two cooperative units (two-state transitions): T_1=50.4 and T_2=51.7°C and the ratio of the relative sizes of thermally labile domains ≅1:2 as judged by $\Delta H_2/\Delta H_1 \cong 2$. The values of T_1 and T_2 agreed with values obtained for Trp and Tyr exposures in N- and C-terminal domains, respectively (Fig. 1). The same DSC data could be fitted equally well by assuming two sequential two-state transitions [13]. From these results, we concluded that thermally-induced partial unfolding of the Mn·GS dodecamer involves two thermodynamic domains. Since different structural domains of each subunit are involved in Trp and Tyr exposures, we could further conclude that partial unfolding reactions in subunit domains are linked so that all subunits within the dodecamer cooperatively undergo partial unfolding. The specific enthalpy for thermally induced transitions of Mn·GS is only ~1.4 J g^{-1}, as compared to the value of 59±17 J g^{-1} determined for the complete dissociation and unfolding of Mn·GS in urea [17], and would not have been detected in the absence of a high

degree of cooperativity during partial unfolding. Remarkably, the thermally induced partial unfolding reactions led to a fully populated intermediate state along the unfolding pathway of dodecameric GS [18].

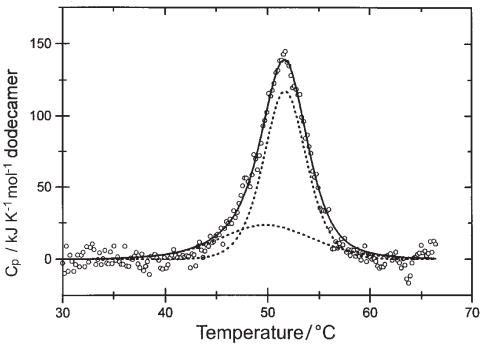

Fig. 2 Deconvolution analysis of DSC data for the partial unfolding of dodecameric Mn·glutamine synthetase in the presence of 1 mM free Mn^{2+}, pH 7.0 (T_m=51.5°C; ΔH=766 kJ mol^{-1}). A random model for two independent two-state transitions (dotted curves) and their sum (solid curve) are shown. A model for two sequential two-state transitions also was fitted to the DSC data and gave an overall fit similar to that shown by the solid line for the random model. Parameters of the random (sequential) model were T_m^1=50.4 (50.2)°C; ΔH=289 (335) kJ mol^{-1} and T_m^2 =51.7 (51.7)°C; ΔH=610 (525) kJ mol^{-1}. Data are from [13, 14], using a MC-2 DSC from MicroCal, Inc.

Thermal unfolding of *Acanthamoeba* myosin II

Myosin II from *Acanthamoeba castellanii*, a conventional myosin similar to mammalian skeletal muscle myosin, is composed of a pair of heavy chains (M_r ~172 000) and two pairs of light chains (M_r ~17 500 and 17 000) [19, 20]. The N-terminal regions of the heavy chains form globular heads while the C-terminal domain forms an α-helical, coiled-coil rod [21, 22]. Each of the two myosin heads contain a nucleotide and an actin binding site and this amino acid sequence is similar to that of muscle myosin [22]. However, the amino acid sequence of the myosin II rod cannot be aligned with the rod sequences of other myosins, although it contains the same periodic repeats of hydrophobic and charged residues found in other coiled-coil structures [22]. Also, the myosin II rod is considerably shorter than that of skeletal muscle myosin (~90 *vs.* 160 mm [23, 24]) and it contains regulatory phosphorylation sites (3 seryl residues/chain) in the unstructured C-terminal tail region [25].

Zolkiewski conducted the DSC studies shown in Fig. 3 with intact *Acanthamoeba* myosin II and skeletal muscle myosin prepared by Redowicz under nonfilamentous conditions [26]. Substantial differences between the DSC profiles for myosin II and rabbit skeletal muscle myosin were observed. The latter unfolds over a wider temperature range (i.e., less cooperatively), which suggests that there are differences in both the number and properties of the thermodynamic domains of these

myosins. In the absence of nucleotide, T_m=41.7°C with ΔH=4500 kJ mol^{-1} for myosin II and T_m=46.3 and 53.7°C with an overall ΔH of 10 500 kJ mol^{-1} for skeletal muscle myosin [26, 27]. The DSC data were only slightly affected by scan rates, which indicate that the parameters obtained approximate the reversible steps in unfolding reactions [28, 29]. The enthalpies of thermal unfolding of intact myosins were estimated to correspond to ~70–75% of complete unfolding [26]. Due to the non-repeatability after heating to 70°C and the possible influence of aggregation, deconvolution of DSC data for intact myosin, HMM and S-1 is unreliable [26, 30, 31]. However, the rod domains reversibly unfold with chain dissociation and the pioneering studies of Privalov and colleagues [32] on the reversible unfolding of the mammalian myosin rod and its proteolytic fragments demonstrated the presence of six cooperative unfolding domains in the rod. In contrast, as will be shown below in Fig. 4, the *Acanthamoeba* myosin II rod reversibly unfolds in a single two-state process with concomitant chain dissociation [33].

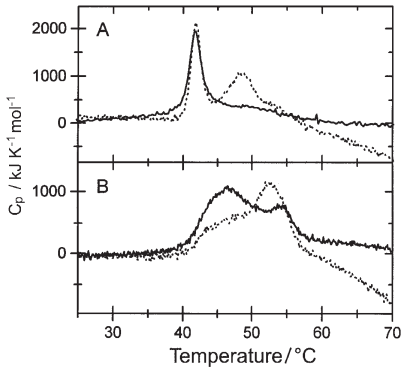

Fig. 3 DSC data for (A) – dephospho-myosin II (1.2 mg ml^{-1}) and; (B) – rabbit skeletal muscle myosin (1.0 mg ml^{-1}) in 10 mM imidazole-HCl, 600 mM KCl, and 1 mM dithiothreitol, pH 7.5 in the absence (solid lines) and presence (dotted lines) of 5 mM Mg^{2+} and 5 mM AMPPNP at scan rates of 60°C h^{-1} (A) and 90°C h^{-1} (B) after subtracting buffer base lines and normalization for protein concentration and scan rate [26]

The function of myosin is to convert the energy of ATP hydrolysis into a directed movement of myosin filaments against actin filaments. The X-ray crystallographic data of Rayment *et al.* [34, 35] support a model, as do also in vitro motility assays with S-1 [36], in which conformational changes in the myosin head are coupled to ATP binding and the release of ADP and phosphate to generate the power stroke. Thermal stabilization of myosin II head domains was greatest with the nonhydrolyzable ATP analogue AMPPNP (Fig. 3a), less with ADP+phosphate, and still less with ADP alone [26]. It was found that the T_m of myosin II heads was insensitive to increasing concentrations of saturating Mg·AMPPNP, which suggests that unfolding reactions are coupled to a nucleotide-induced conformational change [26]. As in the case of *Acanthamoeba* myosin II, Mg·AMPPNP produced changes in the shape of the DSC profile for skeletal muscle myosin (Fig. 3B). The protein post-transitional baseline was more affected by aggregation in

the presence of AMPPNP (Figs 3A and B). Nucleotide also has been shown to stabilize a head fragment of myosin II [26], and HMM [31] and isolated S-1 [31, 37] from skeletal muscle myosin.

The *Acanthamoeba* myosin II rod is a long α-helical coiled-coil with a flexible hinge containing a helix-breaking proline. The thermal stability of the complete rod domain of myosin II (residues 849–1509), a mutant in which the hinge proline was replaced by alanine (P398A), and a mutant with the whole hinge deleted ($\Delta_{384–408}$) was studied under monomeric conditions (0.6 and 2.2 M KCl, pH 7.5) [33]. In analytical ultracentrifuge studies, the purified myosin II rods sedimented as monodisperse dimers with sedimentation coefficients consistent with prolate ellipsoids having an effective length of 82 nm for the wild-type rod and 90 nm for both mutants [33]. The fact that the wild-type rod ellipsoid is effectively shorter is consistent with a bend in the coiled-coil seen in electron microscopy due to the hinge flexibility [22].

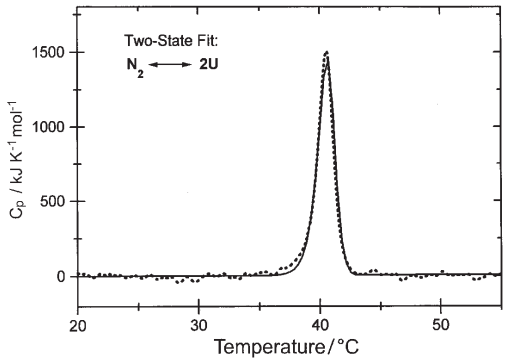

Fig. 4 DSC scan of the *Acanthamoeba* myosin II rod (0.86 mg ml^{-1}) at 7.5°C h^{-1} in 10 mM imidazole, 600 mM KCl, pH 7.5 using a Nano-DSC (from Calorimetry Sciences Corp.), after subtraction of the instrument baseline and a linear baseline connecting pre- and post-transition regions and normalization of the data for scan rate and protein concentration [33]. DSC data (●●●) fitted to a model $N_2 \leftrightarrow 2U$ (coiled-coil dimer↔unfolded chain with c_0=11.5 μM chain) is shown by the solid line; T_m=40.5°C and ΔH=2700 kJ mol^{-1} rod

DSC and circular dichroism (CD) showed that the thermal unfolding of the myosin II rod is reversible and highly cooperative (Fig. 4). The unfolding of the myosin II rod is coupled to a dissociation of chains, as shown by HPLC size exclusion chromatography as a function of temperature and by the protein concentration-dependence of the transition temperature [33]. The CD and DSC data are consistent with a two-state mechanism in which the dimeric rod unfolds with concomitant formation of two unfolded monomers. Figure 4 shows the DSC profile for 5.75 μM rod at a scan rate of 7.5°C h^{-1} together with the fit to a two-state thermodynamic model in which the unfolding of the rod is coupled to chain dissociaton with no intermediate states populated at equilibrium [33]: $N_2 \leftrightarrow 2U$ where N_2 and U are the dimeric, coiled-coil rod and the unfolded chain, respectively. For the data in Fig. 4 (which were obtained

in imidazole buffer at pH 7.5), T_m=40.5°C and ΔH=2700 kJ mol^{-1} rod. Equilibrium CD measurements gave about the same T_m value, but a lower ΔH of ~1700 kJ mol^{-1} due to buffer deprotonation in the DSC experiments [33].

The importance of making measurements under conditions of thermodynamic equilibrium, the significance of which has frequently been ignored or underestimated, was illustrated in thermal unfolding studies of myosin II rods [33]. At a given protein concentration, T_m values were dependent on scan rate (with the temperature of the thermal transition increasing from 40 to 42°C at heating rates of 10 to 50°C h^{-1}, respectively [33]) because the approach to equilibrium was slow, due, most probably, to the dissociation/association of the two polypeptide chains during the unfolding/refolding reactions. A complete recovery of the native conformation after heating and cooling rod samples showed that no irreversible reactions had taken place which could contribute to the apparent kinetic control of unfolding [28]. Non-equilibrium produced by too rapid heating was found to introduce errors in T_m and ΔH values, and accurate determination of T_m values at different protein concentrations is critical for assessing chain dissociation [33].

No deviation from a two-state unfolding was found for the wild-type and mutant myosin II rods. The only difference observed in the unfolding of the wild-type and mutant myosin II rods was a 2°C increase in the thermal stability of the deletion mutant. Thus, the existence of a flexible region in a coiled-coil is not necessarily sufficient to establish independent stable subdomains. (Of course, transient kinetic intermediates can still exist without significantly populating partially unfolded states at equilibrium.) The two-state thermal unfolding of the myosin II rod (with accompanying chain dissociation) implies that separated chain α-helices are thermodynamically unstable at all temperatures under the buffer conditions used. This unfolding behaviour is similar to that of short coiled-coils which contain the leucine zipper motif [38]. Coiled-coil sequences contain periodic seven-residue repeats in which the first and fourth residues are occupied by hydrophobic amino acids, and hydrophobic contacts between the latter stabilize the superhelical complexes of α-helices in the coiled-coil structure.

Thermal unfolding of enzyme I of the *E. coli* PTS

The widespread bacterial phosphoenolpyruvate (PEP):sugar phosphotransferase system (PTS) couples the translocation and phosphorylation of many sugars. The system is composed of two cytoplasmic proteins (enzyme I and HPr) that are used for all sugars as well as sugar-specific, membrane-associated components known as enzymes II. Phosphoenolpyruvate is the high-energy phosphoryl donor in the Mg^{2+}-dependent autophosphorylatin of enzyme I on histidine 189 (with energy retention), and phospho-enzyme I reversibly transfers its phosphoryl group to histidine 15 of HPr [39].

Thermal stabilities of enzyme I (63 562 M_r subunit), in the *E. coli* PTS, and a cloned amino-thermal domain of enzyme I (EIN, 1-258+Arg, 28 346 M_r [40]) were investigated by DSC and far-UV CD at pH 7.5 [41]. EIN expressed in a Δpts strain showed a single, reversible, two-state transition with T_m=57°C and an unfolding enthalpy of 580 kJ mol^{-1} (Fig. 5A). The latter result was similar to results reported by

Chauvin *et al*. [42] for a slightly longer EIN construct (1-268 with a C-terminal Cys added). In contrast, monomeric EIN (containing no Cys or Trp) expressed in a wild-type strain (pts^+) in DSC had two endotherms with $T_m \cong 50$ and 57°C and overall ΔH=570 kJ mol^{-1}, and was converted completely to the more stable form after five DSC scans from 10 to 75°C (Fig. 5B). The far-UV CD spectra, which indicated ~58% helices, was the same for EIN expressed in either Δpts or pts^+ strains [41]. Thermal conversion of the EIN form with a T_m of ~50°C to a more stable form (with T_m=57°C) was correlated with dephosphorylation of this protein by mass spectral analysis [41]. Since EIN can be reversibly phosphorylated in vitro by phospho-HPr but cannot be autophosphorylated by Mg-PEP [40], it was concluded that EIN was partially phosphorylated in vivo when expressed in the wild-type strain [41].

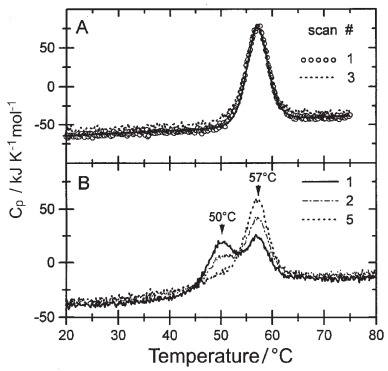

Fig. 5 DSC profiles of EIN (1-258+Arg) at scan rate of 60°C h^{-1} in a MC-2 DSC (from MicroCal, Inc.) with 1.0 mg ml^{-1} protein in 10 mM K–PO_4, pH 7.5 after subtraction of instrument baselines and normalization of the data for protein concentration [41]. (A) – EIN was expressed and purified from a Δpts strain of *E. coli* and three consecutive scans from 10 to 75°C were performed: first scan (DSC data, open circles) and fit to a two-state unfolding model with a progress baseline for $\Delta C_p \geq 0$ (heavy line) and the third scan (dotted line); (B) – EIN was expressed and purified from a wild-type strain (pts^+) and five consecutive scans 15 to 80°C (with rapid cooling and equilibration at 15°C for 1 h between scans) were performed; shown are 1st scan (solid line), 2nd scan (dash-dot line), and 5th scan (dotted line), with decreasing amplitude at 50°C and increasing amplitude at 57°C for scans 1–5 and with the overall enthalpy change constant

EIN proteins with Ala or Glu substituted for the active-site His 189 (H189A and H189E) recently have been cloned, expressed, and purified [43]. Introduction of Ala or the negatively charged Glu at position 189 produced ~2 or 4°C destabilization, respectively, in DSC and CD measurements [43].

The X-ray crystallographic structure of dephospho-EIN (1-258+Arg) determined by Liao *et al*. [44] showed that the protein has two distinct subdomains: one contains four α-helices arranged as two hairpins and the second consists of three- and four-stranded antiparallel and parallel β sheets, respectively, together with three short α-helices. The active-site His 189 is buried between the α- and α/β-subdomains of EIN and hydrogen-bonded to Thr 168. The NMR solution structures of the dephos-

pho- and phospho-forms [45, 46] confirmed the crystal structure and the idea that, upon phosphorylation, His 189 rotates toward the surface (breaking the hydrogen bond to Thr 168) for phosphotransfer to HPr. The thermal destabilization of EIN(H189E) compared to the wild-type protein suggests that the EIN(H189E) conformation is more similar to that of phospho-EIN than to dephospho-EIN. However, the destabilization by phosphorylation or substitution of His 189 by Ala or Glu occurs without any loss in secondary structure elements that contribute to the far-UV ellipticity. A proposal of Meijberg *et al*. [47] that hydration of the phosphoryl group will lead to protein destabilization from disruption of water structure may provide a partial explanation of our results. Moreover, the reversible, thermal unfolding of dephospho- or phospho-EIN or EIN(H189A or H189E) is a two-state process, which means that there is cooperative unfolding of the two structural subdomains of EIN without detectable intermediates in each case.

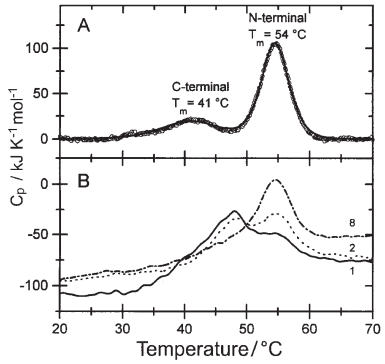

Fig. 6 Thermal unfolding of intact enzyme I in 10 mM K–PO_4, pH 7.5 [41]. (A) – Normalized DSC scan of dephospho-enzyme I (0.14 mg ml^{-1}) at a scan rate of 30°C h^{-1} using the VP-DSC from MicroCal, Inc. After substraction of a linear base line between pre- and post-transition regions, a two two-state fit of DSC data (open circles) to a model for two independent unfolding transitions with the indicated T_m values is shown by the solid line; (B) – Excess heat capacity plots of consecutive DSC scans of partially phosphorylated enzyme I (0.15 mg ml^{-1}), as in (A) at a scan rate of 60°C h^{-1}. Shown are first (solid line), second (dotted line), and eighth (dash-dotted line) scans and the progressive increase in the endotherm area (and peak amplitude) with $T_m \cong 54$°C and corresponding decrease in the peak amplitude of the endotherm with $T_m \cong 47$°C

The DSC profile for intact, dephosphorylated enzyme I (after normalization and subtraction of a base line constructed from pre- and post-transition base lines) is shown in Fig. 6A. Endotherms for the unfolding of the C- and N-terminal domains of enzyme I had T_m values of 41 and 54°C and ΔH values of 240 and 600 kJ mol^{-1}, respectively [41]. The two tryptophanyl residues of enzyme I are in the C-terminal domain and thermally induced fluorescence changes due to Trp exposure gave a perfect fit to a model for a single two-state transition with $T_m \cong 41$°C [41]. Also, thermally-induced ellipticity changes at 222 nm occurred at both DSC endotherms. A sat-

isfactory fit of DSC and CD data to a model of two independent two-state transitions was obtained [41]. Thermal unfolding of the C-terminal domain occurred over a 20°C range and was scan rate-dependent whereas the N-terminal domain unfolding was more cooperative (occurring over a 10°C range) and was scan-rate independent. Repeated DSC scans from 10 to 70°C in the experiments of Fig. 6A gave the same area of the high-temperature endotherm, whereas the low-temperature endotherm gradually disappeared.

Normalized excess heat capacity plots for partially phosphorylated enzyme I of first, second, and eighth scans are shown in Fig. 6B. DSC scans 1 through 8 showed a progressive increase in the endotherm area (and peak amplitude) with $T_m \cong 54$°C and a corresponding decrease in the peak amplitude of the endotherm with $T_m \cong 47$°C. The phosphorylated N-terminal domain masked the unfolding endotherm of the C-terminal domain, as monitored by Trp fluorescence changes [41]; Fig. 6A. The shift in the pre-transition base line in Fig. 6B suggests that some aggregation occurred due to denaturation of the C-terminal domain. The T_m values of 47 and 54°C for partially phosphorylated enzyme I were ~3°C lower than those observed with partially phosphorylated EIN in the same buffer (Fig. 5B). Thus, both phosphorylated and non-phosphorylated N-terminal domains of intact enzyme I are energetically less stable than in the isolated amino-terminal domain. These observations indicate that interactions between the N- and C-terminal domains of enzyme I occur, as proposed by LiCalsi *et al*. [48].

Enzyme I exists in a monomer ↔dimer equilibrium. With a dimerization constant of $\sim 1.7 \cdot 10^4$ (M monomer)$^{-1}$ at 20°C [41], however, <5% dimer was present at the concentration of enzyme I used for the DSC experiment of Fig. 6A. The enthalpy for C-terminal domain unfolding obtained at 0.14 mg ml^{-1} of enzyme I was ~50% of that previously reported by LiCalsi *et al*. [48] for a 10-fold higher protein concentration (and higher ionic strength). When the concentration of enzyme I was increased 3-fold over that used in the experiment of Fig. 6A, the area of the low-temperature endotherm was increased 1.3-fold whereas the enthalpy change for N-terminal domain unfolding was unchanged. This suggests that dimerization stabilizes additional structures in the C-terminal domain, which may relate to the proposal of Roseman and colleagues [39] that dimerization is necessary for the Mg^{2+}-dependent autophosphorylation of enzyme I by PEP.

In summary, thermodynamic information (and especially T_m values) on the thermal unfolding of the amino-terminal domain of enzyme I are sensitive to detecting conformational perturbations produced by phosphorylation. In a related case, Huffine and Scholtz [49] replaced His 15 of HPr from Bacillus subtilus with the negatively charged glutamyl residue to mimic phospho-His 15 and showed that this produced a significant decrease in the conformational stability of the protein, as measured by urea denaturation at 25°C. By using both NMR and molecular dynamics refinement, Van Nuland *et al*. [50] detected a phosphorylation-induced torsion angle strain in the His 15 backbone of HPr that is released upon phosphoryl transfer. This led to the proposal that phosphotransfer from phospho-HPr enzyme II is promoted by the conformational change in HPr [50]. Our finding that enzyme I is destabilized by phospho-

rylation supports and extends this idea, consistent with a phosphorylation- dephosphorylation cycle favoring unidirectional passage of the phosphoryl group from PEP to enzymes II and finally transport of available sugars across the membrane.

References

1 E. R. Stadtman and A. Ginsburg, Enzymes (3rd Ed.), 10 (1974) 755.
2 S. G. Rhee, P. B. Chock and E. R. Stadtman, Adv. Enzymol., 62 (1989) 37.
3 A. Ginsburg, Adv. Protein Chem., 26 (1972) 1.
4 G. Colombo and J. J. Villafranca, J. Biol. Chem., 261 (1986) 10587.
5 R. C. Valentine, B. M. Shapiro and E. R. Stadtman, Biochemistry, 7 (1968) 2143.
6 R. J. Almassy, C. A. Janson, R. Hamlin, N. H. Xuong and D. Eisenberg, Nature, 323 (1986) 304.
7 M. M. Yamashita, R. J. Almassy, C. A. Janson, D. Cascio and D. Eisenberg, J. Biol. Chem., 264 (1989) 17681.
8 J. B. Hunt, P. Z. Smyrniotis, A. Ginsburg and E. R. Stadtman, Arch. Biochem. Biophys., 166 (1975) 102.
9 J. B. Hunt and A. Ginsburg, J. Biol. Chem., 255 (1980) 590.
10 H.. B. Pinkofsky, A. Ginsburg, I. Reardon and R. L. Heinrikson, J. Biol. Chem., 259 (1984) 9616.
11 J. J. Villafranca, D. E. Ash and F. C. Wedler, Biochemistry, 15 (1976) 536.
12 A. Shrake, M. T. Fisher, P. J. McFarland and A. Ginsburg, Biochemistry, 28 (1989) 6281.
13 A. Ginsburg and M. Zolkiewski, Biochemistry, 30 (1991) 9421.
14 M. Zolkiewski and A. Ginsburg, Biochemistry, 31 (1992) 11991.
15 E. M. Freire and R. L. Biltonen, Biopolymers, 17 (1978) 463.
16 E. M. Freire and R. L. Biltonen, Biopolymers, 17 (1978) 481.
17 M. Zolkiewski, N. J. Nosworthy and A. Ginsburg, Protein Sci., 4 (1995) 1544.
18 N. J. Nosworthy and A. Ginsburg, Protein Sci., 6 (1997) 2617.
19 H. Maruta and E. D. Korn, J. Biol. Chem., 252 (1977) 6501.
20 T. D. Pollard, W. F. Stafford, III and R. M. E. Porter, J. Biol. Chem., 253 (1978) 4798.
21 M. A. L. Atkinson and E. D. Korn, J. Biol. Chem., 261 (1986) 3382.
22 J. A. Hammer, III, B. Bowers, B. M. Paterson and E. D. Korn, J. Cell. Biol., 105 (1987) 913.
23 T. D. Pollard, J. Cell. Biol., 95 (1982) 816.
24 A. D. McLachlan, Annu. Rev. Biophys. Bioeng., 13 (1984) 167.
25 C. Ganguly, I. C. Baines, E. D. Korn and J. Sellers, J. Biol. Chem., 267 (1992) 20900.
26 M. Zolkiewski, M. J. Redowicz, E. D. Korn and A. Ginsburg, Arch. Biochem. Biophys., 318 (1995) 207.
27 M. Zolkiewski, M. J. Redowicz, E. D. Korn and A. Ginsburg, Biophys. Chem., 59 (1996) 365.
28 E. Freire, W. W. van Osdol, O. L. Mayorga and J. M. Sanchez-Ruiz, Annu. Rev. Biophys. Chem., 19 (1990) 159.
29 J. M. Sanchez-Ruiz, Biophys. J., 61 (1992) 921.
30 A. Bertazzon and T. Y. Tsong, Biochemistry, 28 (1989) 9784.
31 J. W. Shriver and U. Kamath, Biochemistry, 29 (1990) 2556.
32 P. L. Privalov, Adv. Protein Chem., 35 (1982) 1.

33 M. Zolkiewski, M. J. Redowicz, E. D. Korn, J. A. Hammer, III and A. Ginsburg, Biochemistry, 36 (1997) 7876.
34 I. Rayment, W. R. Rypniewski, K. Schmidt-Base, R. Smith, D. R. Tomchick, M. M. Benning, D. A. Winkelmann, G. Wesenberg and H. M. Holden, Science, 261 (1993) 50.
35 I. Rayment, H. M. Holden, M. Whittaker, C. B. Yohn, M. Lorenz, K. C. Holmes and R. A. Milligan, Science, 261 (1993) 58.
36 H. M. Warrick and J. A. Spudich, Annu. Rev. Cell. Biol., 3 (1987) 379.
37 D. I. Levitsky, V. L. Shnyrov, N. V. Khvorov, A. E. Bukatina, N. S. Vedenkina, E. A. Permyakov, O. P. Nikolaeva and B. F. Poglazov, Eur. J. Biochem., 209 (1992) 829.
38 K. S. Thompson, C. R. Vinson and E. Freire, Biochemistry, 32 (1993) 5491.
39 N. D. Meadow, D. K. Fox and S. Roseman, Annu. Rev. Biochem., 59 (1990) 497.
40 Y. J. Seok, B. R. Lee, P.-P. Zhu and A. Peterkofsky, Proc. Natl. Acad. Sci. USA, 93 (1996) 347.
41 N. J. Nosworthy, A. Peterkofsky, S. König, Y.-S. Seok, R. H. Szczepanowski and A. Ginsburg, Biochemistry, 37 (1998) 6718.
42 F. Chauvin, A. Fomenkov, C. R. Johnson and S. Roseman, Proc. Natl. Acad. Sci. USA, 93 (1996) 7028.
43 A. Ginsburg, R. H. Szczepanowski, S. B. Ruvinov, N. J. Nosworthy, M. Sondeij, T. C. Umland and A. Peterkofsky, Protein Sci., 9 (2000) 1085.
44 D.-I. Liao, E. Silverton, Y.-J. Seok, B. R. Lee, A. Peterkofsky and D. R. Davies, Structure, 4 (1996) 861.
45 D. S. Garrett, Y.-J. Seok, D.-I. Liao, A. Peterkofsky, A. M. Gronenborn and G. M. Clore, Biochemistry, 36 (1997) 2517.
46 D. S. Garrett, Y.-J. Seok, A. Peterkofsky, G. M. Clore and A. M. Gronenborn, Protein Sci., 7 (1998) 789.
47 W. Meijberg, G. K. Schuurman-Wolters and G. T. Robillard, Biochemistry, 35 (1996) 2759.
48 C. LiCalsi, T. S. Crocenzi, E. Freire and S. Roseman, J. Biol. Chem., 266 (1991) 19519.
49 M. E. Huffine and J. M. Scholtz, J. Biol. Chem., 271 (1996) 28898.
50 N. A. J. Van Nuland, J. A. Wiersma, D. Van der Spoel, B. L. De Groot, R. M. Scheek and G. T. Robillard, Protein Sci., 5 (1996) 442.